High power wavelength linearly swept mode locked fiber laser for OCT imaging

George Y. Liu[1], Adrian Mariampillai[1], Beau. A. Standish[1], Nigel R. Munce[1], Xijia Gu[2], and I. Alex Vitkin[3]

[1]*Dept. Medical Biophysics, University of Toronto, 610 University Ave, Toronto, Ontario, Canada M5G 2M9*
yliu308@yahoo.com
[2]*Dept. Electrical and Computer Engineering, Ryerson University, Toronto, M3B 2K3, Canada*
[3]*Depts. Medical Biophysics and Radiation Oncology, University of Toronto, 610 University Ave, Toronto, Ontario, Canada M5G 2M9*

Abstract: We report a long coherence length, high power, and wide tuning range wavelength linearly swept fiber mode-locked laser based on polygon scanning filters. An output power of 52.6 mW with 112 nm wavelength tuning range at 62.6 kHz sweeping rate has been achieved. The coherence length is long enough to enable imaging over 8.1 mm depth when the sensitivity decreases by 8.7 dB ($1/e^2$). The Fourier components are still distinguishable when the ranging depth exceeds 15 mm, which corresponds to 30 mm optical path difference in air. The parameters that are critical to OCT imaging quality such as polygon filter linewidth, the laser coherence length, output power, axial resolution and the Fourier sensitivity have been investigated theoretically and experimentally. Since the wavelength is swept linearly with time, an analytical approach has been developed for transforming the interference signal from equidistant spacing in wavelength to equidistant spacing in frequency. Axial resolution of 7.9 μm in air has been achieved experimentally that approaches the theoretical limit.

OCIS codes: (110.4500) Optical coherence tomography; (140.3600) Lasers, tunable

References and links

1. D. Huang, E. A. Swanson, C. P. Lin, J. S. Schuman, W. G. Stinson, W. Chang, M. R. Hee, T. Flotte, K. Gregory, C. A. Puliafito, and J. G. Fujimoto, "Optical coherence tomography," Science **254**, 1178-1181 (1991).
2. W. Drexler, U. Morgner, F. X. Kartner, C. Pitris, S. A. Boppart, X. D. Li, E. P. Ippen, and J. G. Fujimoto, "*In vivo* ultrahigh-resolution optical coherence tomography," Opt. Lett. **24**, 1221-1223 (1999).
3. B. E. Bouma, G. J. Tearney, I. P. Bilinsky, B. Golubovic, and J. G. Fujimoto, "Self-phase-modulated Kerr-lens mode-locked Cr:forsterite laser source for optical coherence tomography," Opt. Lett. **21**, 1839-1841 (1996).
4. X. Li, T. H. Ko, and J. G. Fujimoto, "Intraluminal fiber-optic Doppler imaging catheter for structural and functional optical coherence tomography," Opt. Lett. **26**, 1906-1908 (2001).
5. S. H. Yun, G. J. Tearney, J. F. deBoer, N. Iftimia and B. E. Bouma "High-speed optical frequency-domain imaging," Opt. Express: **11,** 2953-2963 (2003).
6. S. R. Chinn, E. A. Swanson, and J. G. Fujimoto, "Optical coherence tomography using a frequency-tunable optical source," Opt. Lett. **22**, 340-342 (1997).
7. S. H. Yun, G. J. Tearney, J. F. deBoer, and B. E. Bouma, "Removing the depth-degeneracy in optical frequency domain imaging with frequency shifting," Opt. Express **12**, 4822-4828 (2004).
8. M. A. Choma, M. V. Sarunic, C. Yang, and J. A. Izatt, "Sensitivity advantage of swept source and Fourier domain optical coherence tomography," Opt. Express **11**, 2183-2189 (2003).
9. R. Huber, M. Wojtkowski, and J. G. Fujimoto, "Three-dimensional and C-mode OCT imaging with a compact, frequency swept laser source at 1300 nm," Opt. Express **13**, 10523-10538 (2005).
10. W. Y. Oh, S. H. Yun, G. J. Tearney, and B. E. Bouma, "115 kHz tuning repetition rate ultrahigh-speed wavelength-swept semiconductor laser," Opt. Lett. **30,** 3159-3161 (2005).

#96440 - $15.00 USD Received 21 May 2008; revised 13 Aug 2008; accepted 17 Aug 2008; published 26 Aug 2008

11. R. Huber, M. Wojtkowski, K. Taira, J. G. Fujimoto, and K. Hsu, "Amplified, frequency swept lasers for frequency domain reflectometry and OCT imaging: design and scaling principles," Opt. Express **13**, 3513-3528 (2005).
12. R. Huber, M. Wojtkowski, J. G. Fujimoto, "Fourier Domain Mode Locking (FDML): A new laser operating regime and applications for optical coherence tomography," Opt. Express **14,** 3225-3237 (2006).
13. S. H. Yun, C. Boudoux, G. J. Tearney and B. E. Bouma, "High-speed wavelength-swept semiconductor laser with a polygon-scanner-based wavelength filter," Opt. Lett. **28**, 1981-1983 (2003).
14. R. Huber, D. C. Adler, J. G. Fujimoto, "The publication were buffering is introduced to increase sweep rate is: Title: Buffered Fourier domain mode locking: unidirectional swept laser sources for optical coherence tomography imaging at 370,000 lines/s," Opt. Lett. **31**, 2975-2977 (2006).
15. D. C. Adler, R. Huber, and J. G. Fujimoto, "Phase-sensitive optical coherence tomography at up to 370,000 lines per second using buffered Fourier domain mode-locked lasers," Opt. Lett. **32**, 626 (2007).
16. R. Huber, D. C. Adler, V. J. Srinivasan, and J. G. Fujimoto, "Fourier domain mode locking at 1050 nm for ultra-high-speed optical coherence tomography of the human retina at 236,000 axial scans per second," Opt. Lett. **32,** 2049-2051 (2007).
17. B. Bouma, G. J. Tearney, S. A. Boppart, M. R. Hee, M. E. Brezinski, and J. G. Fujimoto, "High-resolution optical coherence tomographic imaging using a mode-locked Ti:Al_2O_3 laser source," Opt. Lett. **20**, 1486-1488 (1995).
18. M. Wojtkowski, V. J. Srinivasan, T. H. Ko, J. G. Fujimoto, A. Kowalczyk, and J. S. Duker, "Ultrahigh-resolution, high-speed, Fourier domain optical coherence tomography and methods for dispersion compensation," Opt. Express, **12,** 2404-2422 (2004).
19. http://www.pofc.com/english/Telecom%20Fiber.htm

1. Introduction

Optical coherence tomography (OCT) [1] is finding widespread applications in biomedical imaging, with micrometer spatial resolution [2, 3] and its Doppler extension can image blood flow with velocity ranging from 0.02 to 100 mm/s [4]. High-speed wavelength-swept light sources have become available, and OCT techniques have been improved with Fourier domain measurements [5-11]. The wavelength tuning range determines the axial spatial resolution, while the time of a complete wavelength scan corresponds to an A-line data acquisition; therefore, the repetition rate of the light sources determinates the imaging frame rate. Yun et al. experimentally reported a high-speed wavelength-swept laser source using a polygon-scanner-based wavelength filter [12]. Approximately 20 mW output power with repetition rates at 115 kHz based on polygon scanner [10] and 370 kHz using scan Fabry-Perot filters [13, 14] have also been achieved experimentally.

For effective lasing, photons are required to have sufficient resonant times within the laser cavity for building up the optical power and narrowing the spectral linewidth through mode competition before being coupled out. This typically requires the laser cavity to be short enough to reduce the optical round-trip time of the resonant photons when the wavelength is swept. However, it is very difficult in practice to build a very short fiber cavity since fiber components are typically tens of millimeters in length and need to be spliced together. This significantly limits the performance of high-speed, wavelength-swept fiber lasers, imposing a trade-off between the wavelength sweep rates versus output power, coherence length and wavelength tuning range [11, 12]. An alternative approach to achieve sufficient resonance for a certain frequency component is to use a long fiber delay line. For a specific speed of the bandpass transmission filter, those frequency components are delayed and pass the filter at the exact time when the transmission of the filter is at the next spectral position. Therefore, the retuned photons are synchronized to the transmission filter. This synchronization technique is called Fourier domain mode locking (FDML) [12-15] and generates short optical pulses in the frequency domain. It is similar to the conventional mode-locked lasers that generate short optical pulses in the time domain.

In this paper, we report on a long coherence length, high power and wide tuning range wavelength-swept mode-locked fiber laser for OCT imaging. An output power of 52.6 mW with 112 nm wavelength tuning range centered at 1320 nm at sweeping rate of 62.6 kHz has been achieved. To the best of our knowledge, this is the most powerful wavelength-swept

#96440 - $15.00 USD Received 21 May 2008; revised 13 Aug 2008; accepted 17 Aug 2008; published 26 Aug 2008

light source reported to date. The coherence length is long enough to enable ranging depth over 8.1 mm with only an 8.7 dB decrease in sensitivity and the Fourier components are still detectable when the ranging depth is over 15 mm. An analytical expression has been developed for transforming the interference signal from equidistant spacing in wavelength (λ-space) to equidistant spacing in frequency (k-space) for fast Fourier transform (FFT). An axial resolution of 7.9 μm in air or 5.8 μm in tissue (assuming the refractive index is 1.3) has been achieved, which approaches the theoretically limit. The laser output power with respect to the driving current, polygon rotation frequency, and axial resolutions have been investigated experimentally.

2. Theory for OCT signal processing

2.1 Coherence length of Laser sources

For a typical fiber Mach-Zehnder interferometer (MZI), as shown in Fig. 1(c), a laser beam is split into two through a 3 dB fiber coupler and each of these beams is then aligned with a fiber collimator and reflected by a mirror. The two reflected beams are re-coupled back into the fiber and meet at the 3 dB fiber coupler to produce an interference signal. The interference signals output from the circulator and the 3 dB coupler have an inversed phase and thus can be measured by a balanced detector with an enhanced sensitivity. The output of the balanced detector can be expressed as

$$I \sim \frac{1}{\Delta\lambda_{fwhm}} \int_{-\infty}^{\infty} f(\delta\lambda) \cdot \cos^2\left(\frac{\pi \cdot 2z}{\lambda} + \phi\right) d(\delta\lambda), \tag{1}$$

where $2z$ is the optical path difference, $\Delta\lambda_{fwhm}$ and $f(\delta\lambda)$ are the instantaneous laser linewidth and its spectral profile, λ is the light wavelength in vacuum, $\delta\lambda = \lambda - \lambda_0$ is the wavelength detuning, λ_0 is the filter center wavelength and ϕ is the initial phase. For a top-hat spectral profile $f(\delta\lambda) = 1$ when $|\delta\lambda| \le \Delta\lambda_{fwhm}/2$ and $f(\delta\lambda) = 0$ when $|\delta\lambda| > \Delta\lambda_{fwhm}/2$, Eq. (1) reduces to

$$x(t) = a(z,t)\cos\left(\frac{4\pi z}{\lambda_0 + \Delta\lambda_{FSR} f_{sweep} t}\right), \tag{2}$$

where the DC component and the initial constant phase ϕ have been neglected for simplicity, $a(z,t) = a_0(t)\mathrm{sinc}(z/d_0)$, $d_0 = \frac{\lambda_0^2}{2\Delta\lambda_{fwhm}}$, $\Delta\lambda_{FSR}$ is the spectral tuning range and f_{sweep} is the sweep frequency. Since $\Delta\lambda_{fwhm} << \lambda$, the sinc function is a slow varying term that is superimposed on the first fast term that produces the interference fringes. When $z = d_0$, the interference fringes disappear and the corresponding path difference $2d_0 = \lambda^2/\Delta\lambda_{fwhm}$ is called the coherence length (d_0 is called coherence depth). For a filter with a Gaussian spectral profile $\exp\left[-4\ln(2)\left(\delta\lambda/\Delta\lambda_{fwhm}\right)^2\right]$, this coherence depth is usually expressed as $d_{Gaussian} = \frac{4\ln 2}{\pi}\frac{\lambda^2}{2\Delta\lambda_{fwhm}}$, which is about 12% smaller than d_0 [17, 18].

2.2 k-space

When the frequency of the light source is not swept linearly with time, an accurate and reliable transformation of the interference output to equidistant spacing in frequency (k-space) is critical for FFT to enable a high axial resolution. For AD converter cards with a clock input for triggering, a MZI is usually employed [11, 12] and extra electronics are therefore required

#96440 - $15.00 USD Received 21 May 2008; revised 13 Aug 2008; accepted 17 Aug 2008; published 26 Aug 2008

to generate a TTL clocking signal. The timing jitter of the clocking signal can be a problem and would seriously degrade the axial resolution. For polygon scanner based wavelength-swept light sources, the wavelength varies highly linearly in time, which offers an analytical approach to convert the interference output to equidistant frequency signal for FFT. Defining a new time stream t' to replace the time variable t in Eq. (2) as

$$t' = \frac{t}{1 - \frac{\Delta\lambda_{FSR} f_{sweep}}{\lambda_0} t}, \tag{3}$$

The Eq. (3) reduces to

$$x(t) = a(z,t)\cos(2\pi f t), \tag{4}$$

where $f = (z/\Delta z_0) f_{sweep}$ is the frequency of the k-spaced signal, $\Delta z_0 = \lambda_0^{\,2}/(2\Delta\lambda_{FSR})$, the constant phase has been ignored for simplicity. To obtain an equal frequency spaced signal $t = \frac{i}{N}\frac{1}{f_{sweep}}$, $i = 1,2,...N$ requires only to re-map the signal with a new time stream of $t' = \frac{i'}{N}\frac{1}{f_{sweep}}$, where N is the total number of samples of the signal, and i' that can be solved by Eq. (3) is usually not an integer and an interpretation operation may be required. Since this is an analytical calculation and interpretation, the processing time is negligible compared to the time required for Fourier transformation. We will demonstrate that this analytical technique can provide a signal with an accurate equidistant spacing in frequency, and therefore, the resolution of the point spread function (PSF) is in good agreement with theoretical calculation.

2.3 Fourier detectable range, sensitivity, and axial resolution

The discrete Fourier transform is commonly expressed as $X(k) = \sum_{i=0}^{N-1} x(t_i) e^{j\left(2\pi\frac{i}{N}k\right)}$, $k = 0,1,2,...$. For a total acquisition time of $T_{sweep} = 1/f_{sweep}$, the Fourier frequency is given by $F_k = k f_{sweep}$, equal to the signal frequency f in Eq. (4). The depth is then obtained as $z = k\Delta z_0$. Clearly, Δz_0 represents the axial step, corresponding to the axial resolution.

Since the Fourier spectrum has two positive and negative Fourier frequency components, the maximum detectable axial range ($z_{\max}$) corresponds to the maximum detectable Fourier frequency that can be obtained when these two opposite Fourier frequencies superimpose at $k = N/2$ as $z_{\max} = N\Delta z_0/2$. This maximum detectable range corresponds to the signal sampling rate of two samples every interference period, which is generally not sufficient to describe a periodical signal accurately, thus resulting in a low signal-to-noise ratio. For $N = 1024$, this Fourier detectable range is about 3.97 mm.

For Fourier transformation, the energy conservation law can be expressed as $\sum_{i=0}^{N-1} |x(t_i)|^2 dt = \frac{1}{N}\sum_{k=0}^{N-1} |X(k)|^2$. When the signal amplitude of Eq. (4) is a constant with respect to time t as $a(z,t) = a_0(z)$, (the top-hat evolution profile), the peak of Fourier sensitivity (or strength) is thus obtained as $|X(k)|^2_{\max} \approx a_0^{\,2}(z)(N/2)^2$. This results in peak sensitivities of 94 and 54 dB, respectively for $N = 10^5$ and 1024 samples when the signal amplitude $a_0(z) = 1.0$. By measuring this peak sensitivity as a function of the depth z, the profile of $a_0(z)$ or the coherence length of the light source can be determined.

#96440 - $15.00 USD Received 21 May 2008; revised 13 Aug 2008; accepted 17 Aug 2008; published 26 Aug 2008

When a signal is shaped with an evolution profile, the signal can be simply treated as a shaping profile multiplying a signal with a top-hat profile. The Fourier transformation is therefore the convolution of the Fourier transforms of the shaping profile and the top-hat profile signal. For a typical Gaussian shaping profile as $\mathrm{Gaussine}(q,t)=\exp\left[-4\ln 2\left(\frac{t}{q/f_{sweep}}\right)^2\right]$, the normalized Fourier sensitivity is thus

$$\left|X(z_F)\right|^2=\left|\exp\left[-4\ln 2\left(\frac{z_F}{u\Delta z_0/q}\right)^2\right]\otimes\mathrm{sinc}\left(\frac{z_F-z}{\Delta z_0}\right)\right|^2, \tag{5}$$

where $\otimes$ indicates a convolution operation, $u=4\ln 2/\pi$, z_F is depth variable converted from the Fourier frequency F, and q is the parameter to describe the width of the Gaussian shaping profile. The sinc function is the Fourier transform of signal with a top-hat profile. Note that when $q\to\infty$, Eq. (5) reduces to top-hat profile as $\mathrm{sinc}^2\left[(z_F-z)/\Delta z_0\right]$. The axial resolution is thus the axial step Δz_0, given by Eq. (4). Simulation shows the side lobes of the sinc profile can be suppressed by the operation of the convolution at the expense of degrading the depth resolution, which is in good agreement with our experimental results.

3. Experiments and results

A broad-bandwidth semiconductor optical amplifier (Covega BOA1017) was used as a laser gain medium. A fiber-optic collimator (OZ Optics, focal length of 10 mm, diameter of 2.2 mm) was used to couple the light between the fiber and the polygon filter. Two achromatic lenses (Thorlabs, AC254-075-C & AC254-040-C) with focal lengths of f_1=75mm and f_2=40 mm were used to construct the confocal telescope system. An 830 line/mm diffraction grating (Newport 53004BK) was the dispersion component. A 72-facet polygon mirror (Lincoln Laser, SA34) was used to sweep the wavelength. By inserting a 3.3 km fiber delay line into a 7 m long ring laser cavity, we could alternate between mode-locked and short cavity lasers operation, respectively, as shown in Fig. 1(a).

The polygon based scanning filter is shown in Fig. 1(b). When a parallel beam is incident on the diffraction grating, the rays with the same wavelengths are diffracted by the grating to the same direction. The diffracted rays are then redirected by the confocal telescope and illuminate the polygon mirror and the end mirror. The end mirror reflects back the light to the polygon mirror and finally couples to the fiber through the fiber collimator to realize resonance. Clearly, only the beam with specific wavelength components at specific time can pass the polygon filter and return to the laser cavity. The maximum wavelength tuning range is the free spectral range ($\Delta\lambda_{FSR}$) that is determined by the number of the polygon facets (N), focal lengths of the two lenses and the grating period (Λ) as $\Delta\lambda_{FSR}=(4\pi/N)\Lambda f_2/f_1$ [10]. Spinning the polygon mirror in clockwise direction produces a positive wavelength tuning in the configuration as shown in Fig. 1(b). The linewidth of the polygon filter was ~ 0.2 nm when the beam was incident at an angle of 69°. In order to synchronize the optical resonance to the polygon scanning filter, the optical round-trip time must match the time between two neighboring sweeping period or its harmonics. The sweeping frequency is then expressed as

#96440 - $15.00 USD Received 21 May 2008; revised 13 Aug 2008; accepted 17 Aug 2008; published 26 Aug 2008

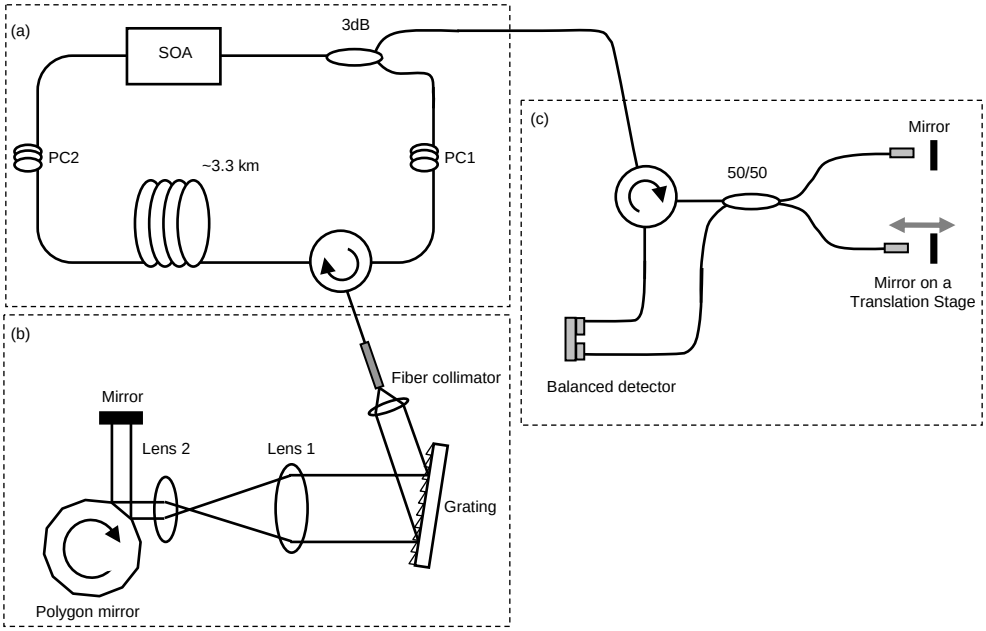

Fig. 1. Schematic diagrams: (a) the frequency domain mode-locked (FDML) wavelength-swept fiber laser, (b) the polygon filer, and (c) The MZI. SOA is the semiconductor optical amplifier, PC1 &2 are polarization controllers.

$$f_{sweep} = M \frac{c}{\mathrm{n}_{eff} L}, (M=1,2,\ldots), \tag{6}$$

where L is the fiber physical length and n_{eff} is the effective refractive index of the fiber core, c is the light velocity in vacuum, and M is the order of the harmonic. In order to reduce the fiber loss and potential dispersion effect, the fundamental mode (M=1) was used in our experiments. Obviously, when the sweeping frequency is tuned around the center mode-locked frequency, the returned photons will mismatch the exact filter wavelength. When this mismatched wavelength is out of the filter wavelength range, no returned photons can pass the filter and the laser is not lasing. The relationship between the sweeping frequency and the filter linewidth is then obtained as

$$\delta\lambda = \Delta\lambda_{FSR} \frac{\delta f}{f_0} \tag{7}$$

where f_0 is the center mode-locked frequency, δf is FWHM of the laser output power profile with respect to the detuning of frequency. For n_{eff} =1.45, L=3.3 km, Eq. (7) gives the mode-locked frequency as f_0=62.70 kHz, which is agreement with our experimental result of 62.57 kHz. Detuning the sweeping frequency from f_0 results in the decrease of the output power, as shown in Fig. 2. For δf =0.11 kHz and $\Delta\lambda_{FSR}$ =112 nm, Eq. (7) gives the filter linewidth as $\delta\lambda$ =0.197 nm, which agrees well with the experimental value of 0.2 nm. The linewidth was measured at the circulator port 3 using an optical spectrum analyzer when the polygon is stationary, where the SOA acted as a wideband light source. Note that the free spectral range is used to represent the wavelength tuning range. This provides a useful way to determine the linewidth of spinning polygon filters. The asymmetry profile as shown in Fig. 2 indicates the wavelength sweeping direction. On average, higher power on the long wavelength side was observed. When the sweeping frequency of the polygon mirror is slightly faster than the

#96440 - $15.00 USD Received 21 May 2008; revised 13 Aug 2008; accepted 17 Aug 2008; published 26 Aug 2008

center mode-locked frequency f_0, the polygon filter will catch up with the wavelength in advance, and thus sweeping direction from short to long wavelength will result in a slow power decrease on average.

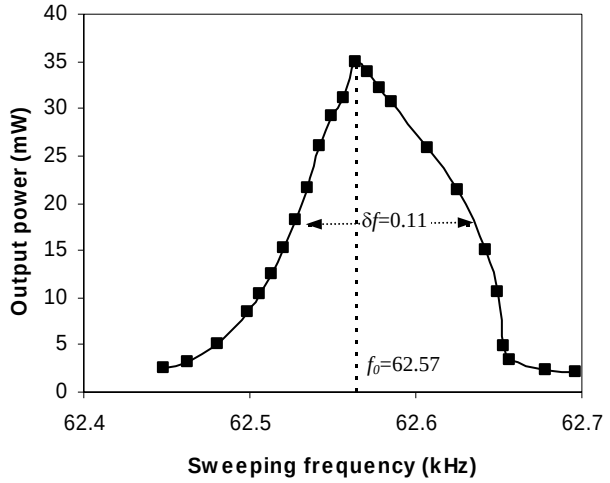

Fig. 2. The frequency domain mode locked (FDML) laser output power as a function of the sweeping frequency, showing f_0=62.57 kHz and δf=0.11 kHz. Squares are experiment data, line is their connection. The asymmetry profile indicates sweeping direction, from short to long wavelengths.

The fiber dispersion effect can be neglected in our experiments. For L=3.3 km fiber with σ=3.1 ps/nm/km dispersion coefficient at 1300 nm band [18], the group delay for $\Delta\lambda$ spectral width is expressed as $dt = \sigma L \Delta\lambda$, 2.05 ps and 1.15 ns, respectively for instantaneous filter linewidth of 0.2 nm and wavelength tuning range of 112 nm, corresponding to the filter wavelength mismatches of 1.4×10^{-5} nm and 8.0×10^{-3} nm at a 62 kHz (f) sweeping frequency ($\Delta\lambda_{FSR}\, fdt$). This is about two orders of magnitude lower than the filter linewidth and hence can be neglected. Note that the second order dispersion with coefficient of 0.085ps/km/nm^2 has the same order magnitude effect compared with the first order.

#96440 - $15.00 USD Received 21 May 2008; revised 13 Aug 2008; accepted 17 Aug 2008; published 26 Aug 2008

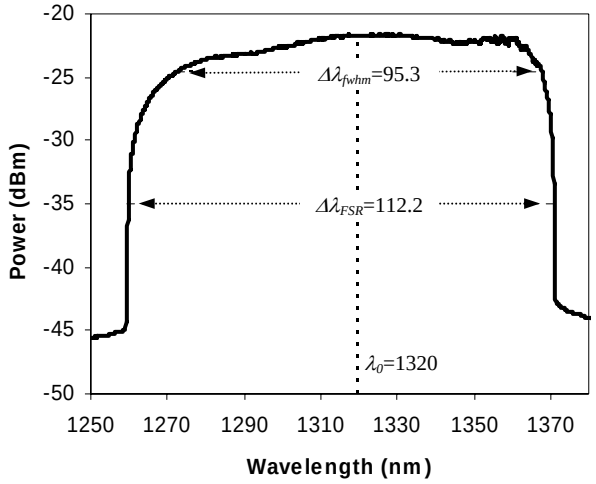

Fig. 3. The spectrum of the FDML laser, showing sweeping range of $\Delta\lambda_{FSR}$=112.2 nm and full width at half maximum of 95.3 nm.

The FDML laser spectrum measured using an optical spectrum analyzer (Ando AQ-6310B) in peak-hold mode is shown in Fig. 3. 112.2 nm tuning range ($\Delta\lambda_{FSR}$) centered at 1320 nm was obtained, which agrees well with the theoretical calculation of 111.7 nm. The full width at half maximum width is approximately 95 nm.

The laser output power with respect to the SOA driving current is shown in Fig. 4. The lasing thresholds for the mode-locked and short cavity lasers are ~100 mA and ~250 mA, respectively. The slope efficiencies for the both laser configurations are almost the same, ~0.134 mW/mA. When the polygon mirror is stationary, the short cavity gives slightly more output power compared to that of the long fiber mode-locked cavity, since the presence of 3.3 km fiber will introduce an additional loss. However, when the polygon is spinning, the mode-locked laser has considerably higher output power and longer coherence length due to the synchronized resonance. Up to 52.6 mW high power has been obtained. Such a large output power level is attractive for OCT, enabling potentially faster imaging or multiple-OCT-probe operation.

#96440 - $15.00 USD Received 21 May 2008; revised 13 Aug 2008; accepted 17 Aug 2008; published 26 Aug 2008

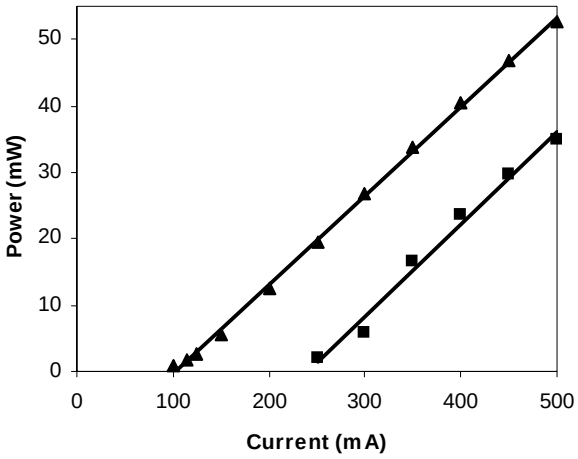

Fig. 4. The output power of the laser as a function of the SOA driving current, showing that the current thresholds for mode locked (triangles) and short cavity lasers (squares) are ~100 mA and ~250 mA, respectively. The slopes for both configurations are the same within experimental error, ~0.134 mW/mA.

Figure 1(c) illustrates the MZI for the measurement of the point spread functions (PSFs) with respect to the reflection depths. The reflection depth can be adjusted by moving a mirror mounted on a translation stage. A balanced detector and an oscilloscope (Tektronix TDS5054B) with 2.5 GS/s sampling rate (500 MHz bandwidth) were used to capture the interference signal. At the depth position of 1.65 mm, the interference signal is shown in Fig. 5. The insert is the zoom-in of the signal to shown the interference fringes.

When this interference signal is shaped to a top-hat and Gaussine$(1/e,t)$ evolution profiles, respectively, the theoretical and experimental PSFs at this depth are shown in Fig. 6(a) and (b). The insert figures in Fig. 6(a) and (b) are used to indicate the signal evolution profiles. The interference frequency in the insert figures is reduced for visual purposes. The FWHM at this depth for top-hat profile is about 7.9 μm, which closes to the 7.8 μm, the theoretical derived limit for a light source with a tuning range of 112.2 nm centered at 1320 nm wavelength. For the Gaussian shaping evolution profile, the signal-to-noise ratio can be improved due to the suppression of the side lobes while the axial resolution degrades to 13.4 μm. The mechanism of this resolution degradation results from the reduced effective tuning range. For a shaping profile of Gaussine$(0.5,t)$, experimental results show the axial resolution is ~10.0 μm. Experimental results are in good agreement with the theoretical calculation.

#96440 - $15.00 USD Received 21 May 2008; revised 13 Aug 2008; accepted 17 Aug 2008; published 26 Aug 2008

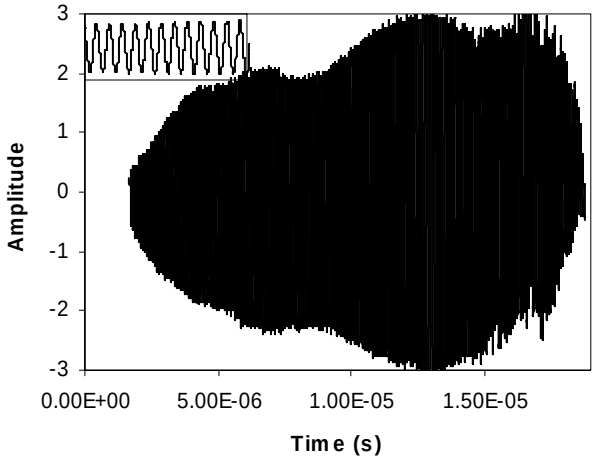

Fig. 5. The interference signal captured by an oscilloscope at a depth of 1.65 mm, corresponding to a path difference of 3.3 mm. The insert is the zoom-in of the interference fringes.

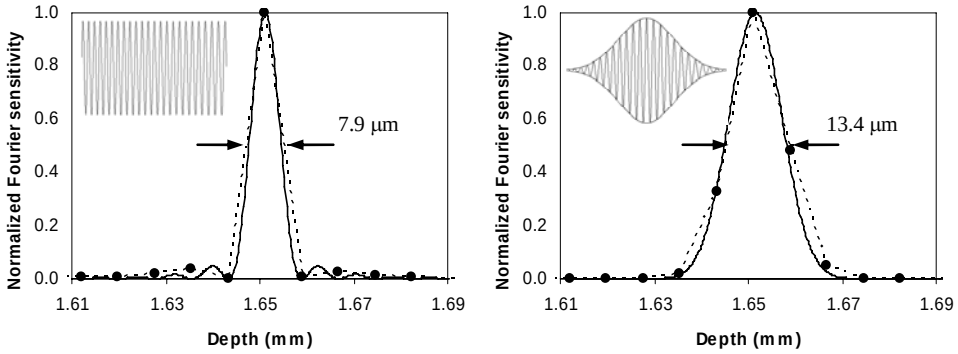

(a) (b)

Fig. 6. The experimental and theoretical PSFs for signal with evolution profiles of (a): Top-hat, (b) $\mathrm{Gaussine}(1/e,t)$. Points are experimental data and dashed curves are their connections. Solid curves are theoretical calculations, showing a 7.9 μm and 13.4 μm FWHM for top-hat and $\mathrm{Gaussine}(1/e,t)$ profiles.

The coherence length of the laser source can be investigated by measuring the peak Fourier sensitivities as a function of the reflection depths. The PSFs at different depths for FDML at the signal sampling rate of 2.5 GS/s is shown in Fig. 7(a). An OCT ranging depth of 8.1 mm, corresponding to 16.2 mm optical path difference in air, with only an 8.7 dB ($1/e^2$) decrease in sensitivity has been achieved in our experiments. Note that the depth is ~7.3 mm for a 7.5 dB sensitivity decrease. The Fourier components are still distinguishable when the ranging depth exceeds 15 mm.

#96440 - $15.00 USD Received 21 May 2008; revised 13 Aug 2008; accepted 17 Aug 2008; published 26 Aug 2008

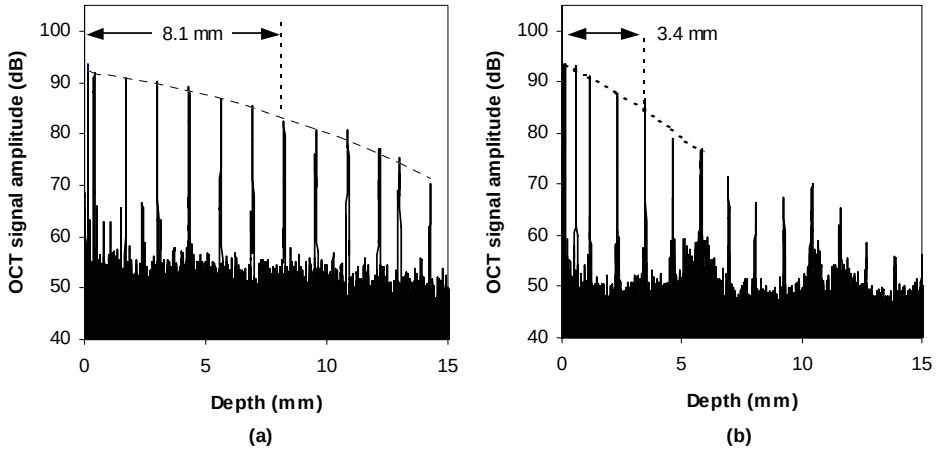

Fig. 7. Measured PSFs at different depths showing the ranging depths are (a) 8.1 mm for a FDML laser, and (b) 3.4 mm for a short cavity laser when the sensitivity decrease by 8.7 dB.

When the FDML laser is switched to a short cavity fiber ring laser by removing the 3.3 km long fiber delay line, the resulting PSFs at different depths are shown in Fig. 7(b). The ranging depth reduces to 3.4 mm when the sensitivity decreases by 8.7 dB at sweeping frequency of 42.9 kHz.

We used an oscilloscope (TDS505B) with signal sampling rate of 2.5 GS/s to capture the interference signal. The samples for an A-scan was $\sim 4\times 10^4$, which is large enough to analyse tens of millimeters in ranging depth for a sweeping frequency of 62.6 kHz. When the signal sampling rate reduces to 100MS/s, the samples reduce to ~1600, corresponding to a maximum Fourier measurable range of ~6.2 mm. When the ranging depth closes to this depth, the signal-noise ratio will be degraded dramatically.

4. Conclusion

We have demonstrated a long coherence length, high power, wide spectral range wavelength-swept fiber mode-locked laser based on a polygon scanning filter. An output power of 52.6 mW with 112 nm wavelength tuning range centered at 1320 nm, 62.6 kHz sweeping rate and 8.1 mm OCT ranging depth with 8.7 dB or $1/e^2$ decrease in sensitivity have been achieved from a single semiconductor optical gain medium and 3.3 km fiber cavity. The Fourier components are still distinguishable at the reflection depth of 15 mm. For a 7 m long short-cavity, the corresponding power and depth drop to 35 mW and 3.4 mm, respectively when the sweeping frequency is 42.9 kHz. The laser thresholds for mode-locked and short-cavity are ~100 mA and ~250 mA while the slope efficiencies are ~0.134 mW/mA. An analytical expression has been developed for calculating of the polygon filter linewidth from the measurement of the power profile width with respect to the sweeping frequency. The asymmetry of this power profile indicates the wavelength sweeping direction. By taking the merit of linear wavelength tuning, an analytical method has been demonstrated to provide an accurate equidistant k-spaced signal. Axial resolution of 7.9 μm in air, approaching the theoretical limit, has also been achieved.

#96440 - $15.00 USD Received 21 May 2008; revised 13 Aug 2008; accepted 17 Aug 2008; published 26 Aug 2008